

Multiresolution Methods

Aiichiro Nakano

*Collaboratory for Advanced Computing & Simulations
Department of Computer Science
Department of Physics & Astronomy
Department of Chemical Engineering & Materials Science
Department of Biological Sciences
University of Southern California*

Email: anakano@usc.edu

Divide-&-conquer in continuum simulations



Discrete vs. Continuum Applications

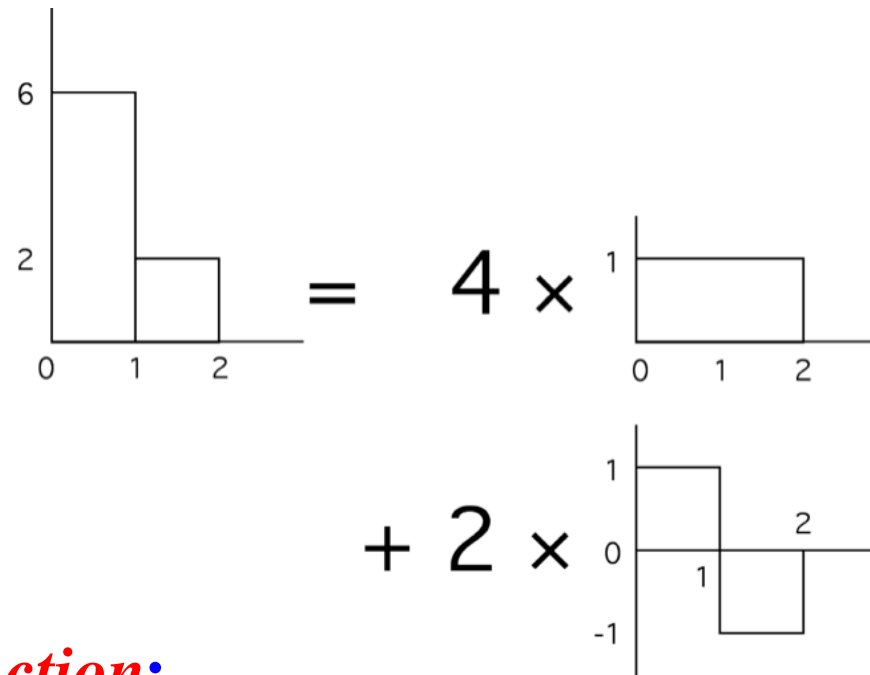


Figure 2. Newton and Schrödinger's cat. Previously, classical physics and quantum chemistry belonged to rivalling worlds. The Nobel Laureates in Chemistry 2013 have opened a gate between those worlds and have brought about a flourishing collaboration.

- Discrete simulation: *e.g.* molecular dynamics (**Newtonian mechanics**)
- Continuum simulation: *e.g.* quantum dynamics (**Schrödinger equation**); *cf.* image processing
- Multiresolution methods in the context of image processing

Haar Wavelet Basis

- One-dimensional “image”: $\mathbf{I}[2] = (6, 2)$
- Smooth component: $s = (6 + 2)/2 = 4$
- Detailed component: $d = (6 - 2)/2 = 2$
- Wavelet decomposition: $\mathbf{I}[] = (6, 2) = 4 \times (1, 1) + 2 \times (1, -1)$



- Haar *scaling function*:
 $\phi(x) = 1 (0 \leq x < 2); 0 (\text{otherwise})$
- Haar *wavelet function*:
 $\psi(x) = 1 (0 \leq x < 1); -1 (1 \leq x < 2); 0 (\text{otherwise})$

Wavelet Decomposition

- One-dimensional “image”:

$I[16] = (1, 2, 5, 9, 1, 9, 2, 2, 2, 3, 5, 7, 4, 2, 1, 1)$

- Smooth component:

$s[i] = (I[2*i] + I[2*i+1])/2 \quad (i=0, \dots, 7)$

- Detailed component:

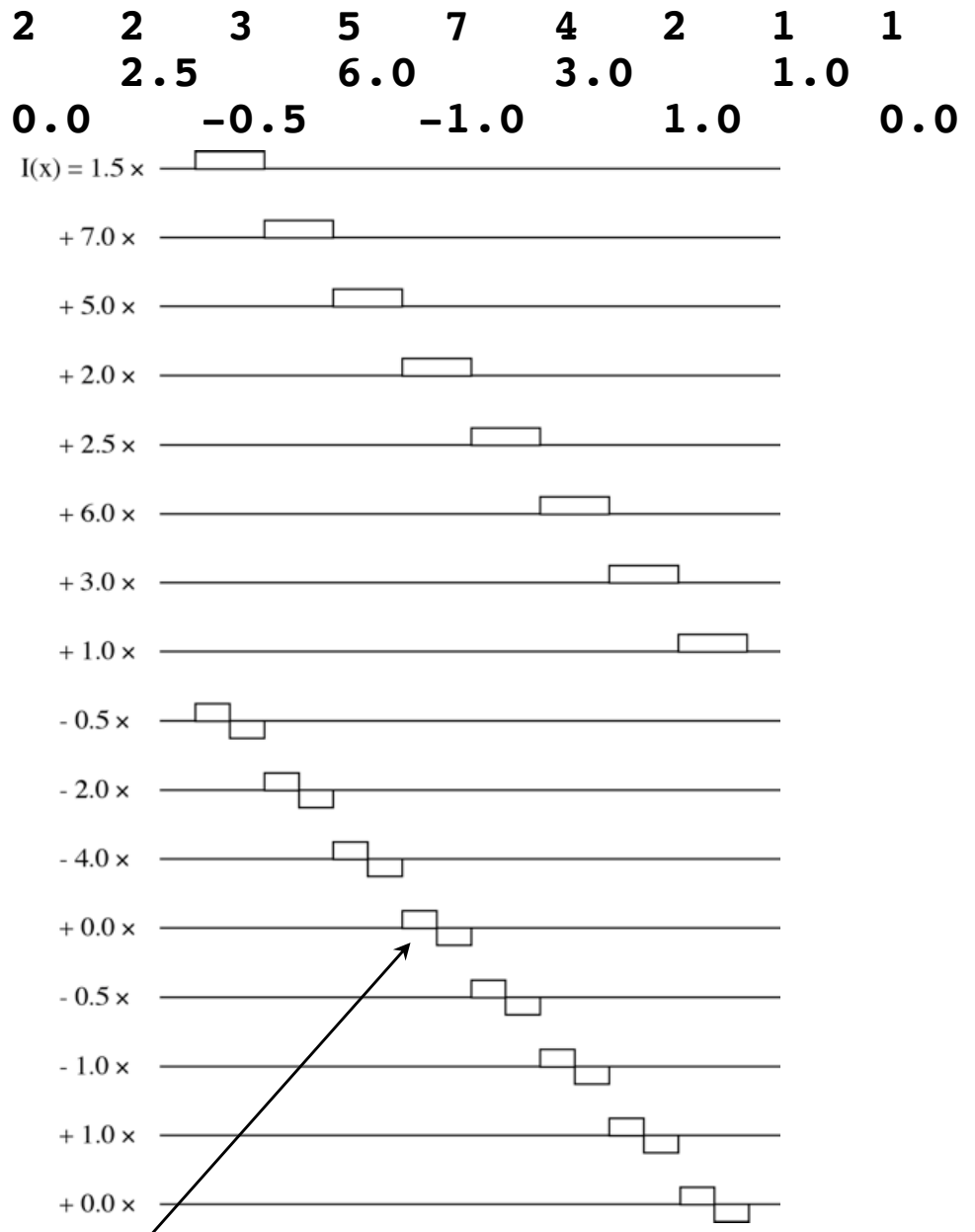
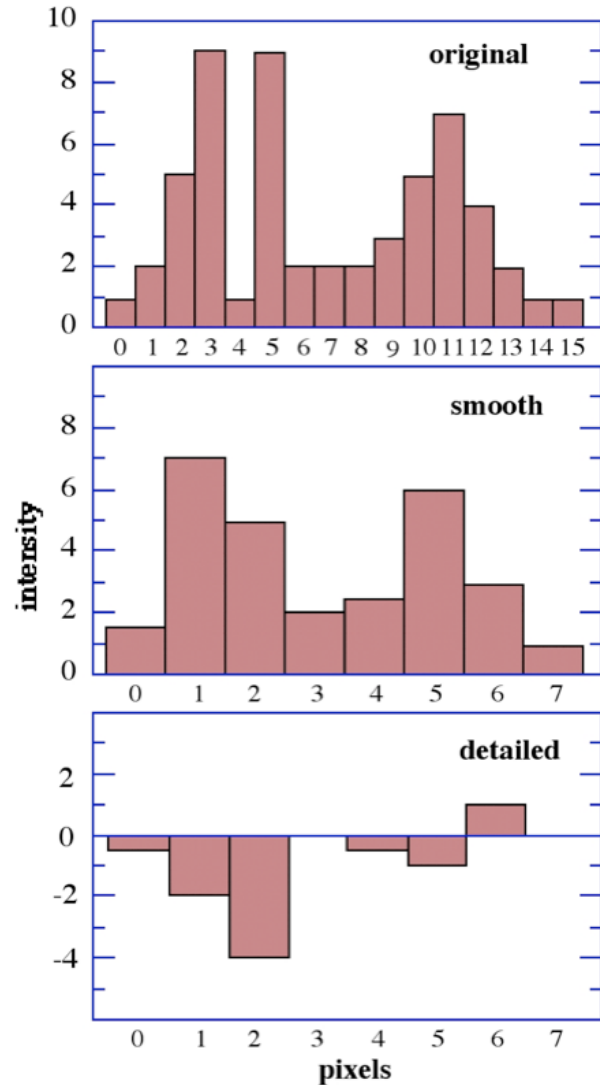
$d[i] = (I[2*i] - I[2*i+1])/2 \quad (i=0, \dots, 7)$

- Wavelet decomposition:

$I[16]$	1	2	5	9	1	9	2	2	2	3	5	7	4	2	1	1
$s[8]$	1.5		7.0		5.0		2.0		0.0		2.5		6.0		3.0	
$d[8]$		-0.5		-2.0		-4.0				-0.5		-1.0		1.0		0.0

Wavelet Decomposition

I[16]	1	2	5	7.0	9	1	5.0	9	2	2	2	3	5	7	4	2	1	1
s[8]	1.5								2.0								1.0	
d[8]				-0.5			-2.0						-0.5		-1.0		1.0	0.0



Wavelets = spatially localized waves also localized in wavenumber

Multiresolution Analysis

- Recursive wavelet decomposition:

$$\mathbf{I}[16] \rightarrow \mathbf{s}[8], \mathbf{d}[8]$$

$$\mathbf{s}[8] \rightarrow \mathbf{ss}[4], \mathbf{sd}[4]$$

$$\mathbf{ss}[4] \rightarrow \mathbf{sss}[2], \mathbf{ssd}[2]$$

$$\mathbf{sss}[2] \rightarrow \mathbf{ssss}[1], \mathbf{sssd}[1]$$

- Recursive vector-subspace decomposition:

$$\mathbf{V}^0 = \mathbf{V}^1 + \mathbf{W}^1; \mathbf{s}[8] \in \mathbf{V}^1; \mathbf{d}[8] \in \mathbf{W}^1$$

$$\mathbf{V}^1 = \mathbf{V}^2 + \mathbf{W}^2; \mathbf{ss}[4] \in \mathbf{V}^2; \mathbf{sd}[4] \in \mathbf{W}^2$$

...

- Multiresolution representation

$$\mathbf{I}[16] \rightarrow \mathbf{d}[8], \mathbf{sd}[4], \mathbf{ssd}[2], \mathbf{sssd}[1], \mathbf{ssss}[1]$$

or

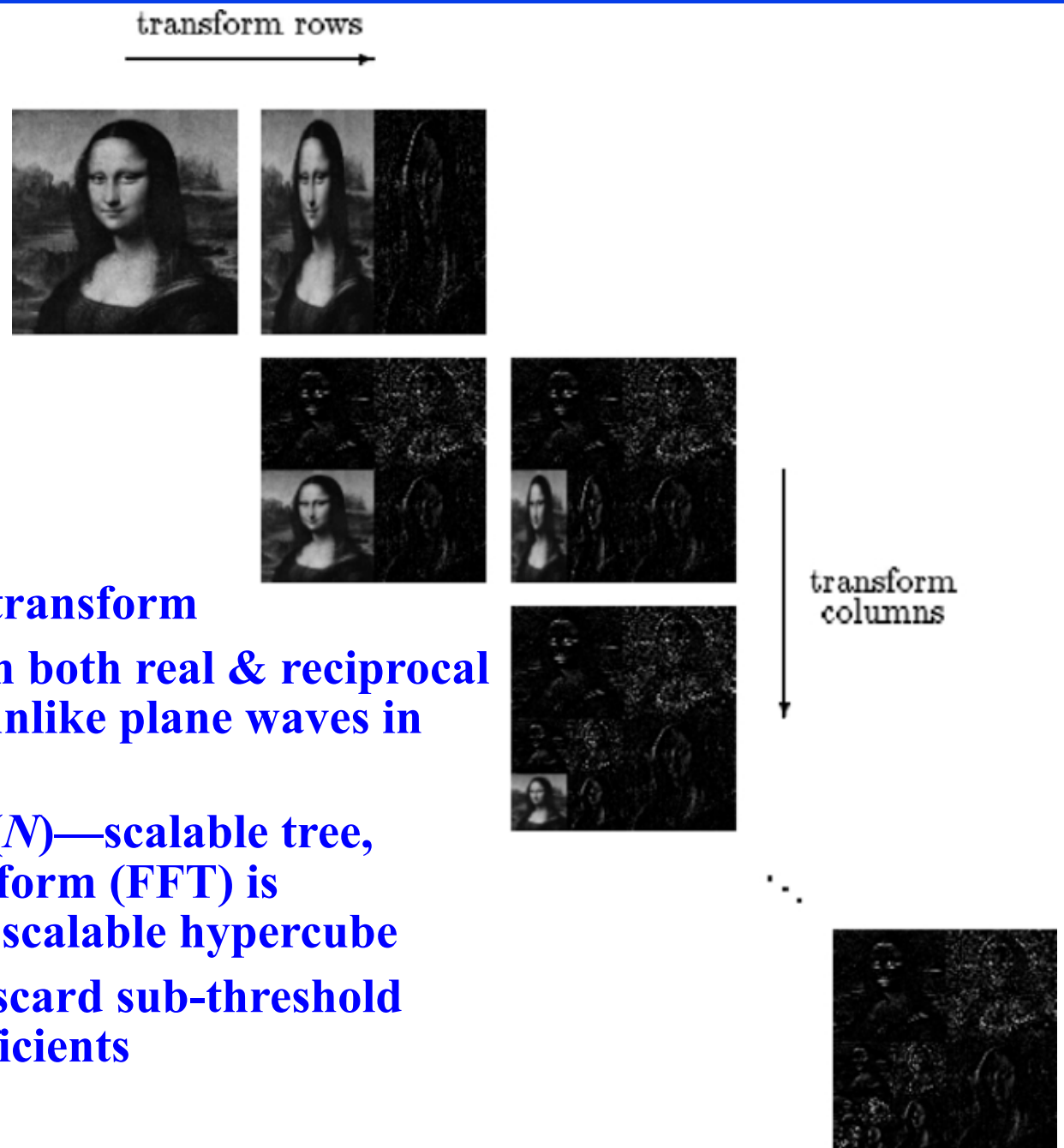
$$\begin{aligned}\mathbf{V}^0 &= \mathbf{V}^1 + \mathbf{W}^1 \\ &= \mathbf{V}^2 + \mathbf{W}^2 + \mathbf{W}^1 \\ &= \mathbf{V}^3 + \mathbf{W}^3 + \mathbf{W}^2 + \mathbf{W}^1 \\ &= \mathbf{V}^4 + \mathbf{W}^4 + \mathbf{W}^3 + \mathbf{W}^2 + \mathbf{W}^1\end{aligned}$$

Very smooth

Progressively more details

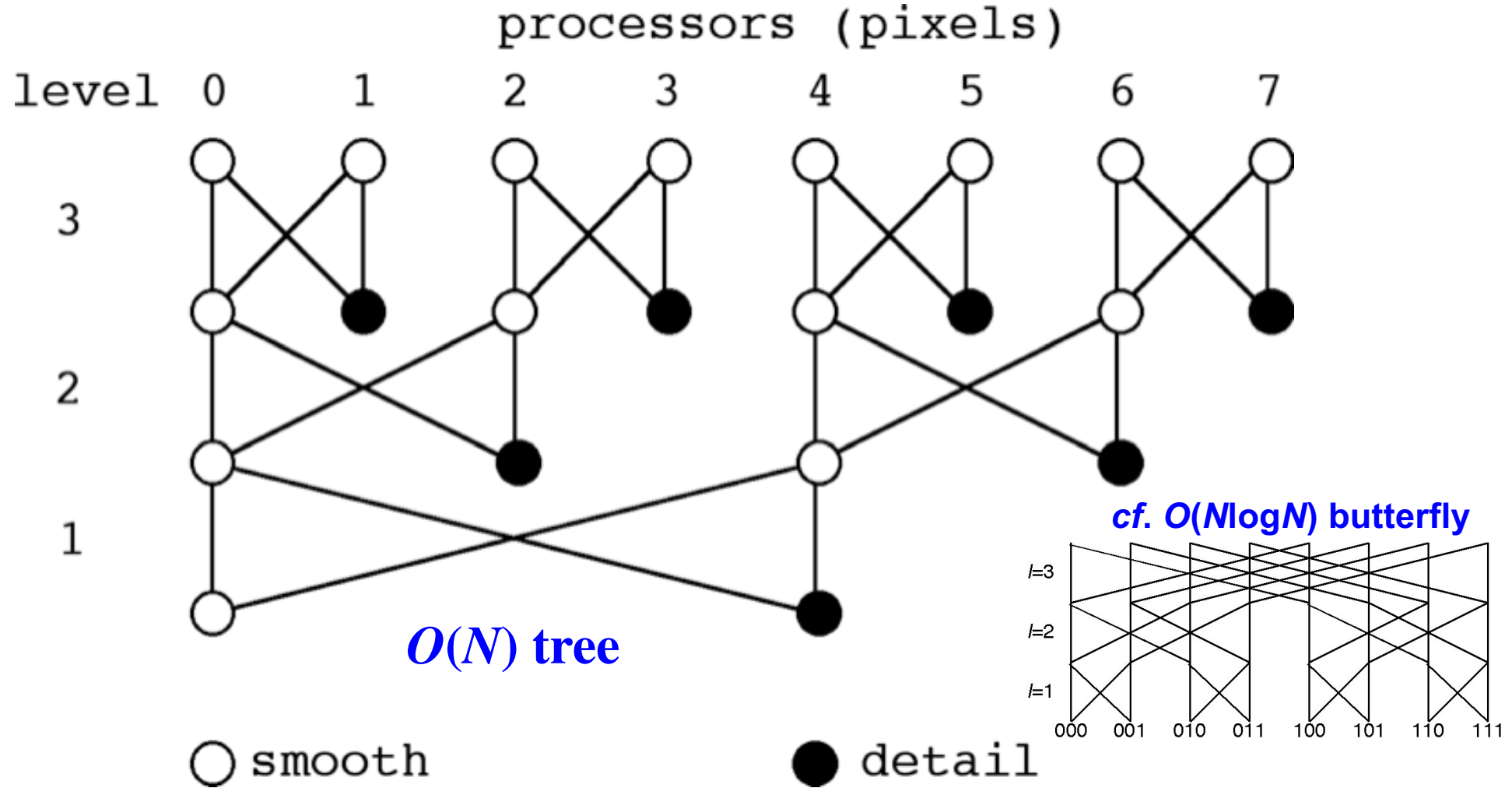
Wavelet Image Decomposition

- Alternate row & column transformations



Parallel Multiresolution Analysis

- Local with spatial decomposition at fine scales
- Subtree masters own coarse smooth components



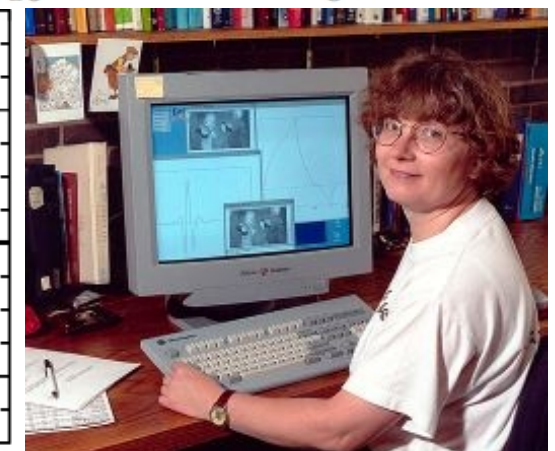
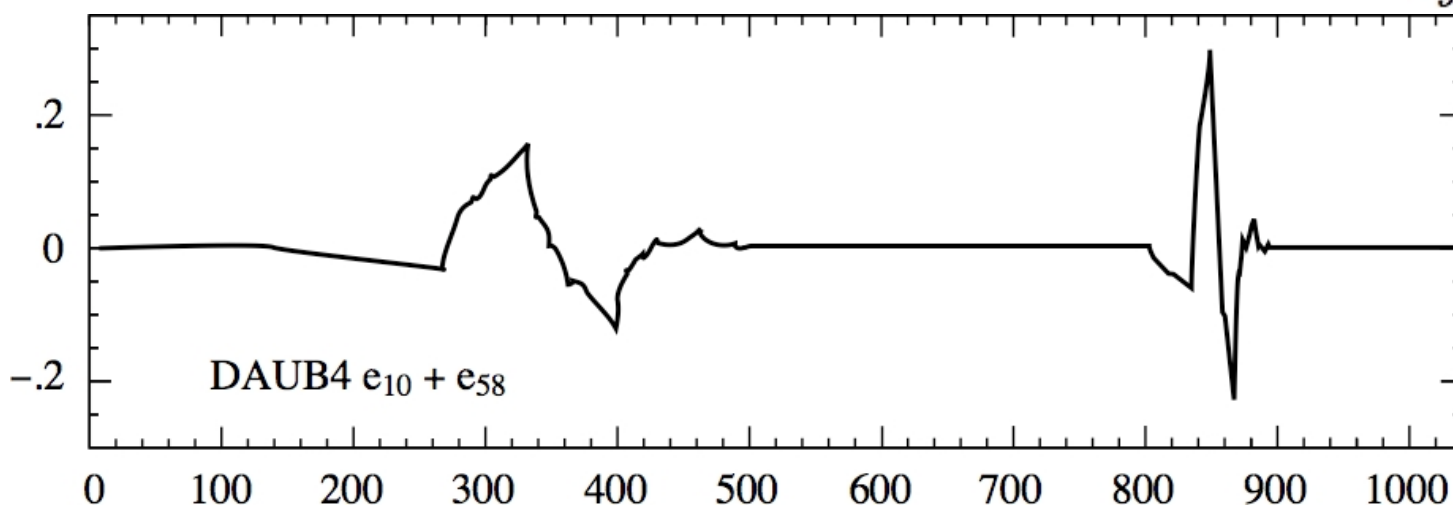
- Retain detailed components? Let subtree slaves do (cf. hypercube quicksort)

Daubechies Wavelets

- Moving window for smooth & detailed filters

$$\begin{array}{c}
 \left[\begin{array}{cccc} c_0 & c_1 & c_2 & c_3 \\ c_3 & -c_2 & c_1 & -c_0 \\ & c_0 & c_1 & c_2 & c_3 \\ & c_3 & -c_2 & c_1 & -c_0 \\ \vdots & \vdots & & & \ddots \\ & & & & c_0 & c_1 & c_2 & c_3 \\ & & & & c_3 & -c_2 & c_1 & -c_0 \\ & & & & & c_0 & c_1 \\ & & & & & c_3 & -c_2 \\ c_2 & c_3 \\ c_1 & -c_0 \end{array} \right] \longrightarrow \left[\begin{array}{c} y_1 \\ y_2 \\ y_3 \\ y_4 \\ y_5 \\ y_6 \\ y_7 \\ y_8 \\ y_9 \\ y_{10} \\ y_{11} \\ y_{12} \\ y_{13} \\ y_{14} \\ y_{15} \\ y_{16} \end{array} \right] \rightarrow \left[\begin{array}{c} s_1 \\ d_1 \\ s_2 \\ d_2 \\ s_3 \\ d_3 \\ s_4 \\ d_4 \\ s_5 \\ d_5 \\ s_6 \\ d_6 \\ s_7 \\ d_7 \\ s_8 \\ d_8 \end{array} \right]
 \end{array}$$

$C_0 = (1 + \sqrt{3}) / 4\sqrt{2} = 0.4829629131445341$
 $C_1 = (3 + \sqrt{3}) / 4\sqrt{2} = 0.8365163037378079$
 $C_2 = (3 - \sqrt{3}) / 4\sqrt{2} = 0.2241438680420134$
 $C_3 = (1 - \sqrt{3}) / 4\sqrt{2} = -0.1294095225512604$



Ingrid Daubechies

Iterative Solution of Linear Systems

$$\mathbf{A} = \mathbf{L} + \mathbf{D} + \mathbf{U}$$
$$\begin{bmatrix} X & & \\ X & X & \\ X & X & X \end{bmatrix} + \begin{bmatrix} X & & \\ & X & \\ & & X \end{bmatrix} + \begin{bmatrix} X & X & X \\ X & X & \\ & & X \end{bmatrix}$$

- Fixed-point equation

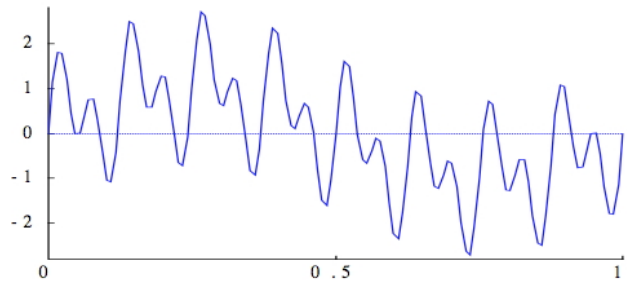
$$\mathbf{x} = \mathbf{D}^{-1}[-(\mathbf{L}+\mathbf{U})\mathbf{x} + \mathbf{b}]$$

- Jacobi iteration

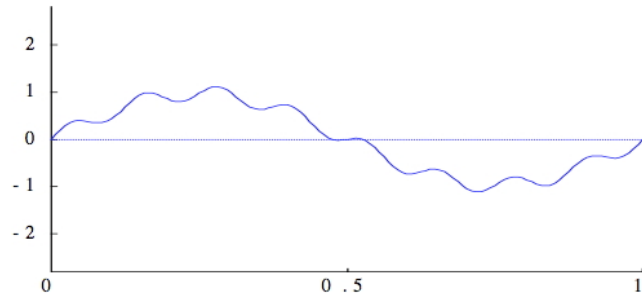
$$\mathbf{x}^{(n+1)} = \mathbf{D}^{-1}[-(\mathbf{L}+\mathbf{U})\mathbf{x}^{(n)} + \mathbf{b}]$$

$$x_i^{(n+1)} = \frac{1}{a_{ii}} \left(- \sum_{\substack{j=1 \\ (j \neq i)}}^N a_{ij} x_j^{(n)} + b_i \right)$$

- Initial error:



- Error after 35 iteration sweeps:



Multigrid Method

- **Residual equation:**

$A^{(l)}$: l -th level matrix
v: Current guess
e: error vector
r: residual vector

$$\begin{aligned} & \text{exact} \\ \overbrace{\quad}^{} \quad A^{(l)} \widehat{(v + e)} &= -4\pi e^2 \mathbf{n} \\ \overbrace{\quad}^{} \quad \Rightarrow A^{(l)} v &= -4\pi e^2 \mathbf{n} + \mathbf{r} \\ & A^{(l)} e = -\mathbf{r} \end{aligned}$$

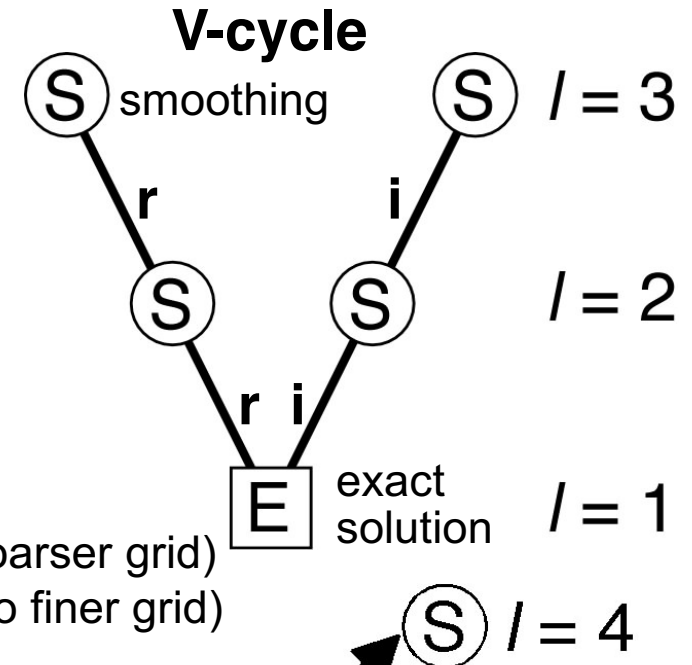
- **Smoothing:**

$$e \leftarrow [1 + Z^{(l)} A^{(l)}] e + Z^{(l)} r$$

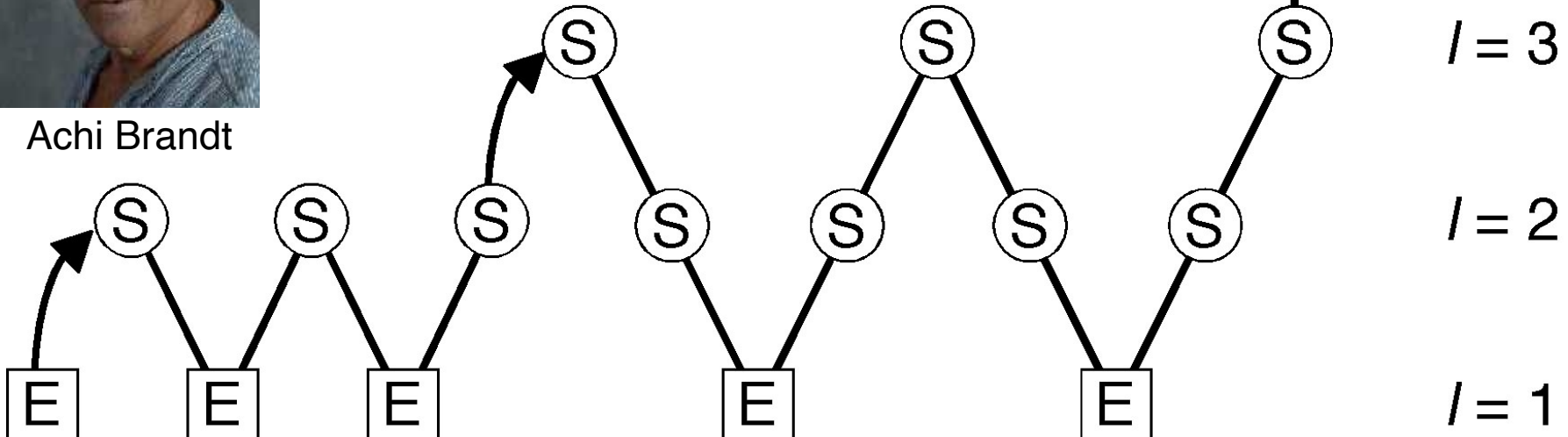
- **Coarsening of residual & interpolation of error**



Achi Brandt

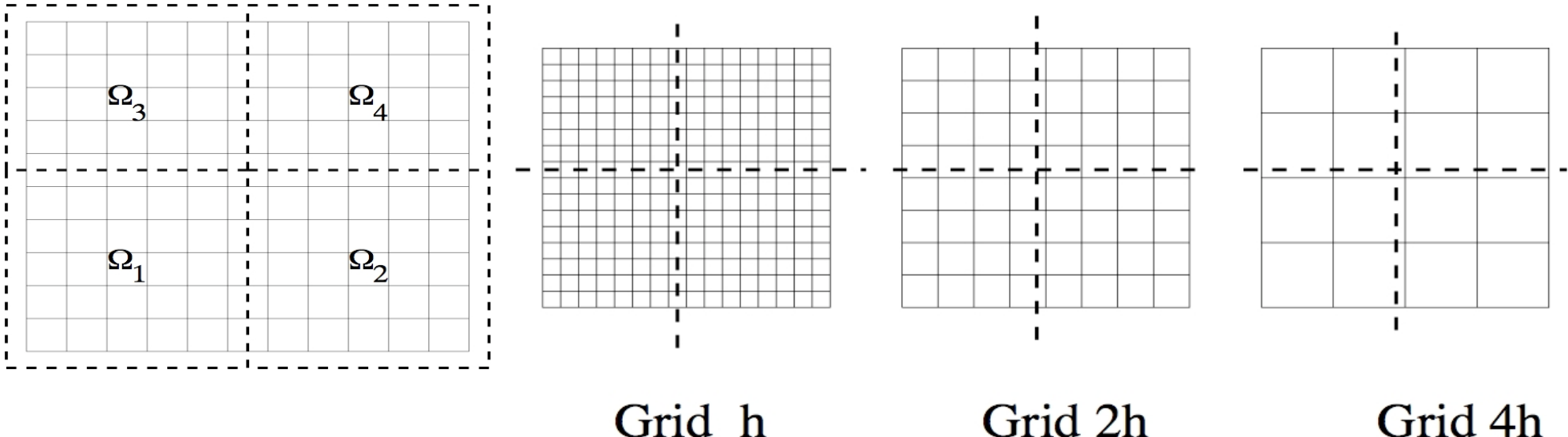


Full multigrid



Parallel Multigrid Method

- Domain decomposition with boundary-layer caching



- 2D computational & communication costs (isogranular or weak scaling)

$N \times N$ grids each on $P \times P$ processors: $T(N^2 P^2, P^2) = a \log NP + bN + cN^2$

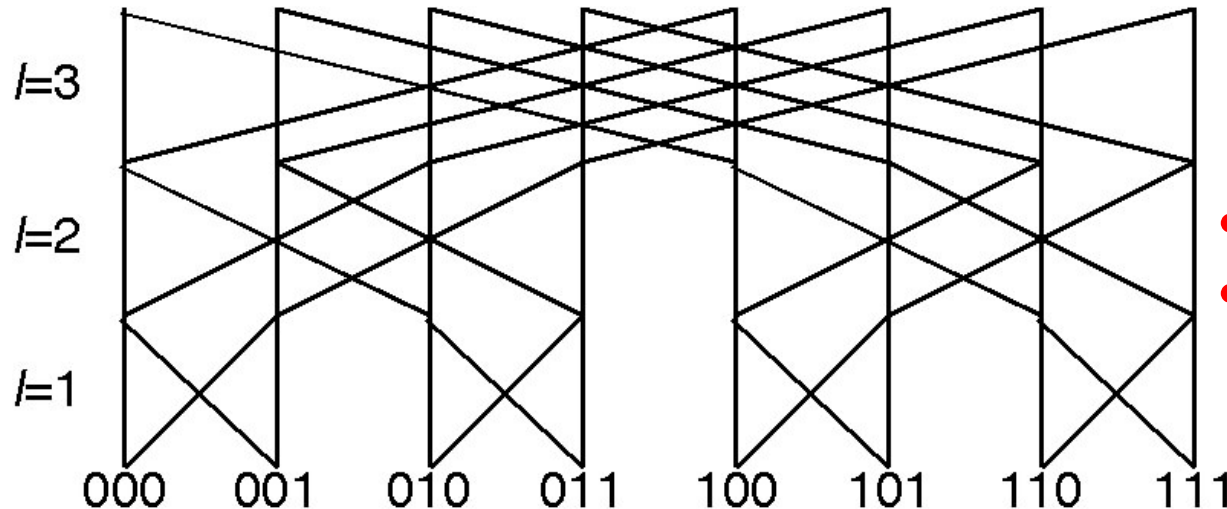
Weak-scaling speedup & efficiency

$$S_{P^2} = \frac{N^2 P^2 T(N^2, 1)}{N^2 T(N^2, P^2)} = \frac{P^2 (cN^2)}{a \log NP + bN + cN^2} = \frac{P^2}{1 + \frac{b}{cN} + \frac{a}{cN} \log NP}$$

$$E_{P^2} = \frac{S_{P^2}}{P^2} = \frac{1}{1 + \frac{b}{cN} + \frac{a}{cN} \log NP}$$

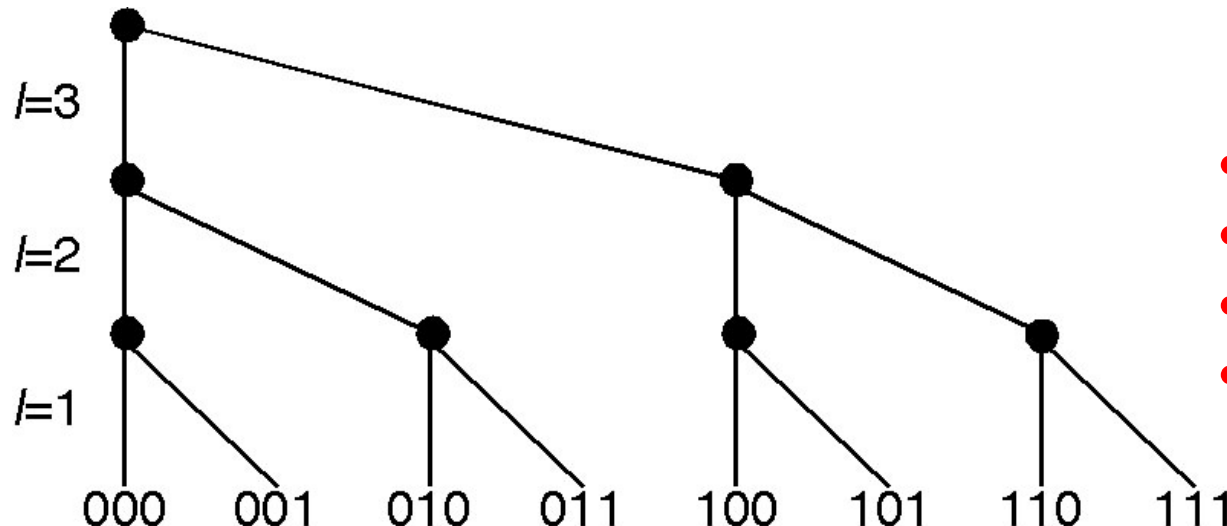
Global Communications

All-to-all (hypercube): $O(N \log N)$



- Quicksort
- Fast Fourier transform

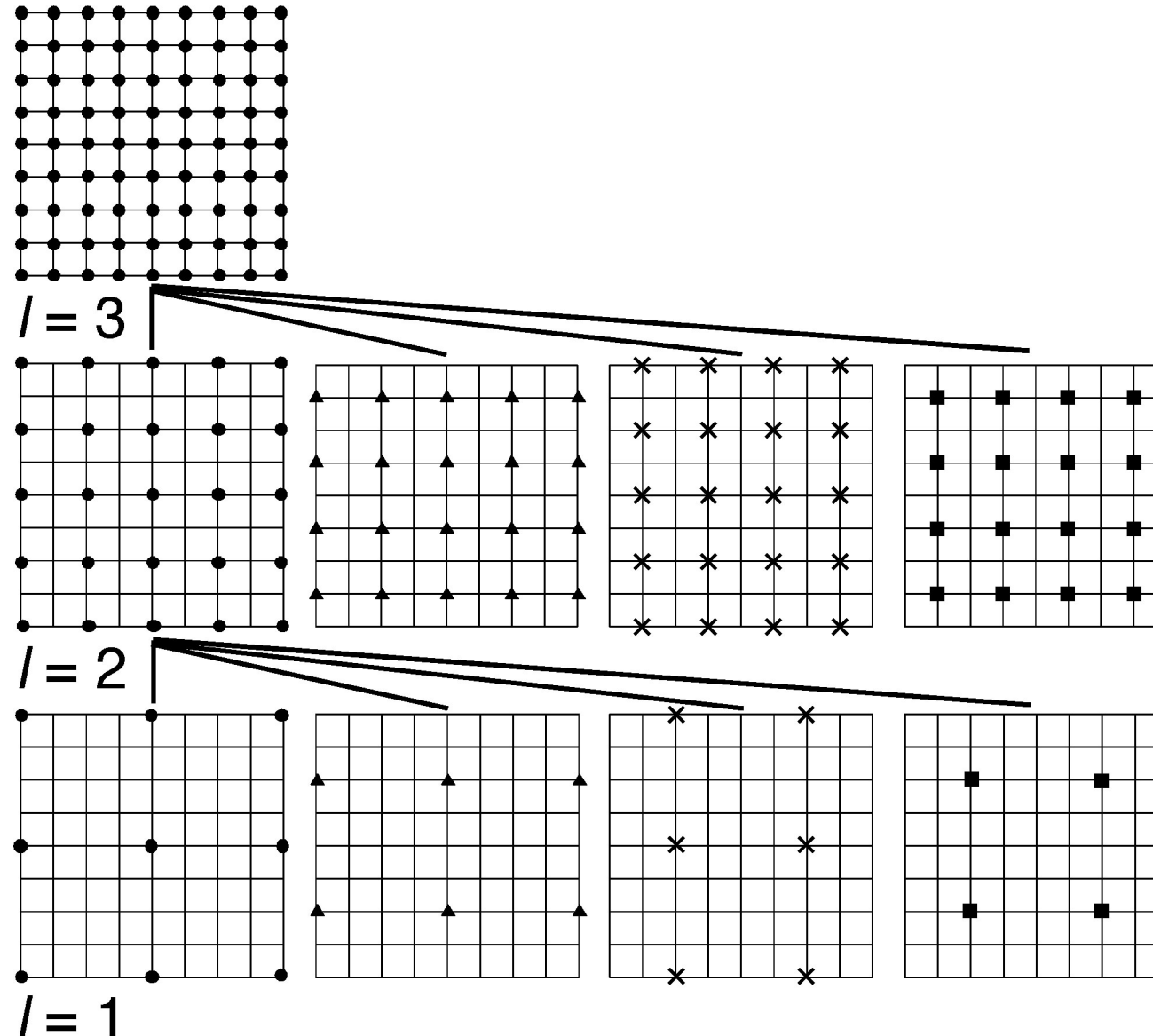
All-to-one (tournament): $O(N)$



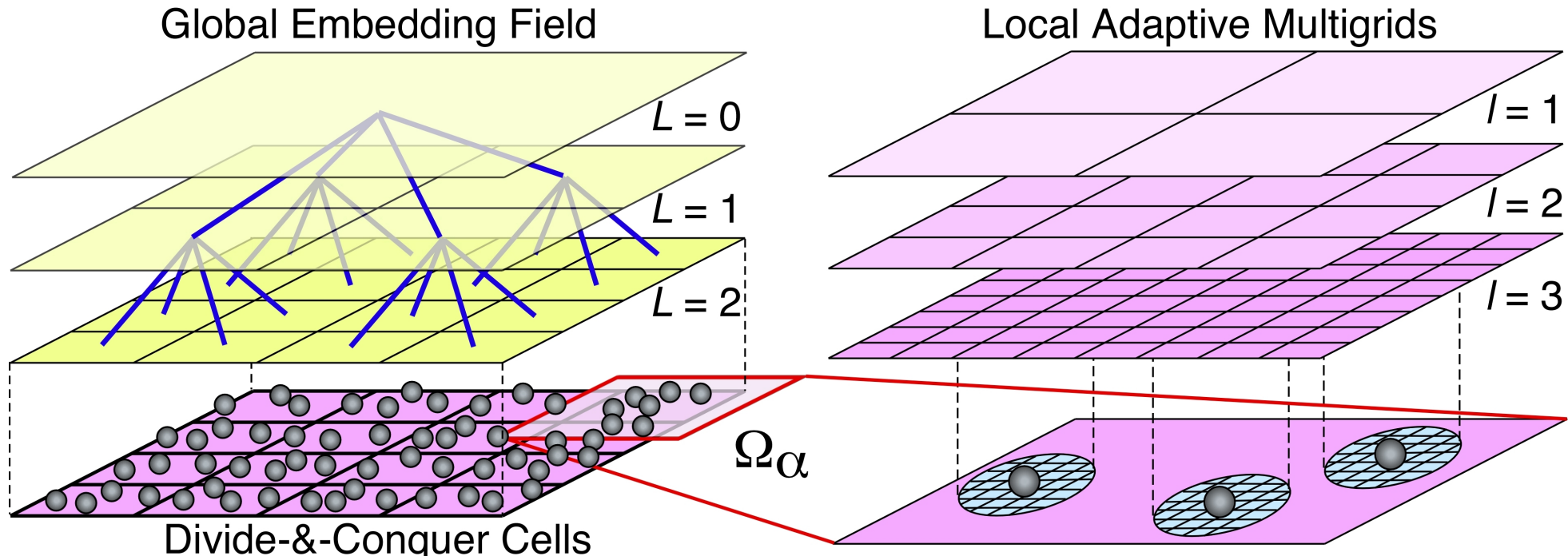
- Global reduction
- Fast multipole method
- Multigrid method
- Wavelets

Solving the Idle Processor Problem

- Parallel superconvergent multigrid: Solve multiple coarse problems to accelerate the convergence [Frederickson & McBryan, '88]



Divide-&-Conquer Algorithms



- **N -body problem:** $O(N^2) \rightarrow O(N)$
 - > **Space-time multiresolution molecular dynamics (MRMD):** Fast multipole method & symplectic multiple time stepping
- **Variable N -charge problem:** $O(N^3) \rightarrow O(N)$
 - > **Fast reactive force-field (F-ReaxFF) MD:** Multilevel preconditioning
- **Quantum N -body problem:** $O(C^N) \rightarrow O(N)$
 - > **DC density functional theory (DC-DFT):** Adaptive multigrids

A. Nakano *et al.*, Int'l J. High Performance Comput. Appl. **22**, 113 ('08)

Molecular Dynamics: N -Body Problem

- Newton's equations of motion

$$m_i \frac{d^2 \mathbf{r}_i}{dt^2} = -\frac{\partial E_{\text{MD}}(\mathbf{r}^N)}{\partial \mathbf{r}_i} \quad (i = 1, \dots, N)$$

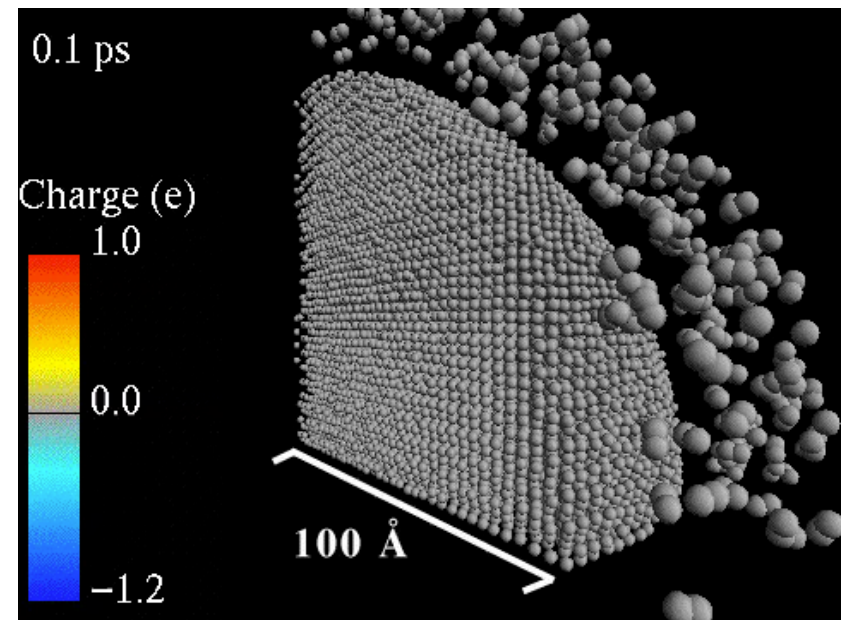
- Reliable interatomic potential

$$E_{\text{MD}} = \sum_{i < j} u_{ij}(r_{ij}) + \sum_{i, j < k} v_{jik}(\mathbf{r}_{ij}, \mathbf{r}_{ik})$$

- N -body problem

Long-range electrostatic interaction — $O(N^2)$

Evaluate $V_{\text{es}}(\mathbf{x}) = \sum_{j=1}^N \frac{q_j}{|\mathbf{x}-\mathbf{x}_j|}$ at $\mathbf{x} = \mathbf{x}_i$ ($i = 1, \dots, N$)



- $O(N)$ space-time multiresolution MD (MRMD) algorithm

1. Fast multipole method (FMM) [Greengard & Rokhlin, '87]
2. Symplectic multiple time stepping (MTS) [Tuckerman *et al.*, '92]

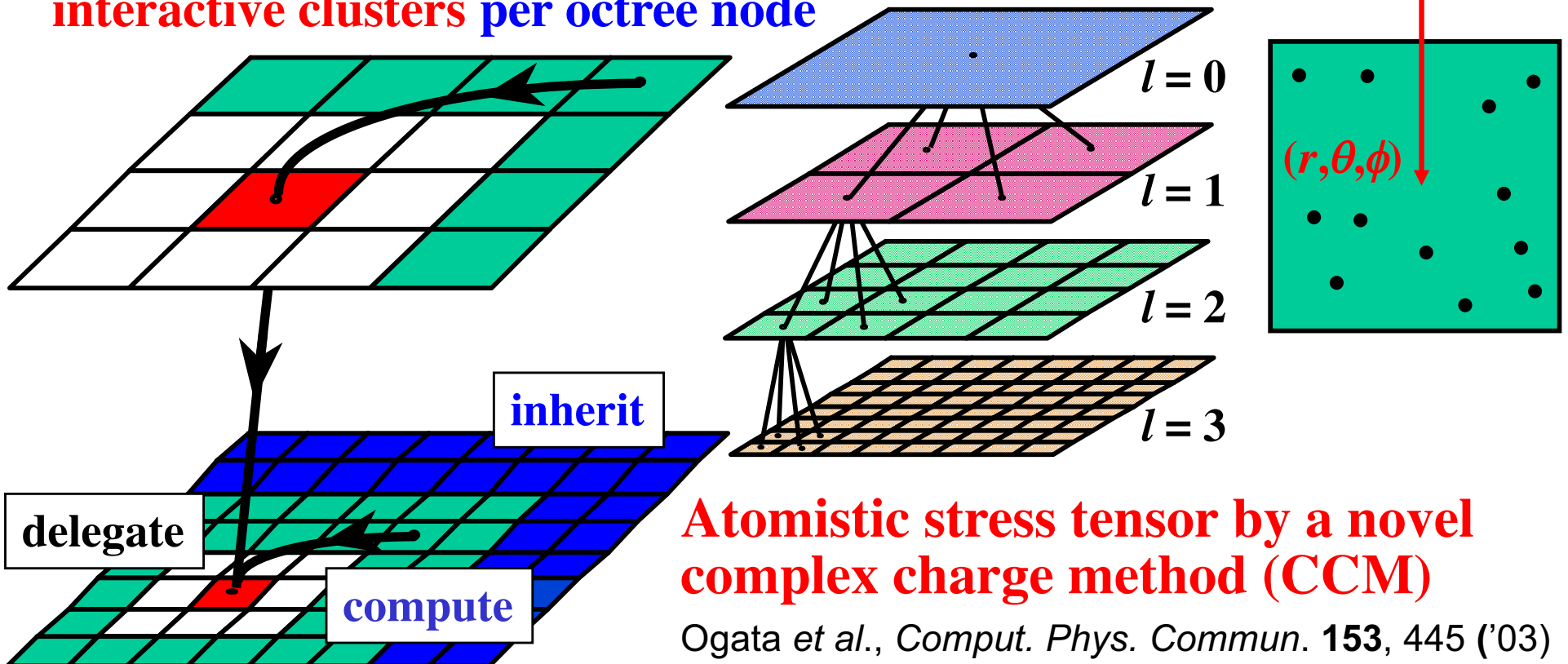
Spatial Locality: Fast Multipole Method

1. Clustering: Encapsulate far-field information using multipoles

$$V(\mathbf{x}) = \sum_{l=0}^{\infty} \sum_{m=-l}^{l} \left\{ \sum_{i=1}^N q_i r_i^l Y_l^{*m}(\theta_i, \phi_i) \right\} \frac{Y_l^m(\theta, \phi)}{r^{l+1}}$$

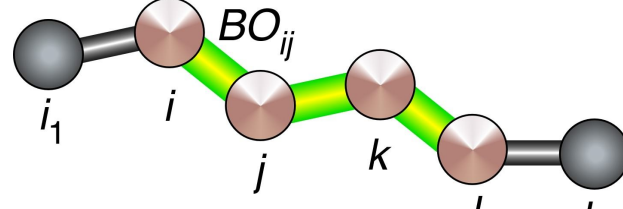
2. Hierarchical abstraction: Octree data structure

3. $O(N)$ algorithm: Constant number of interactive clusters per octree node

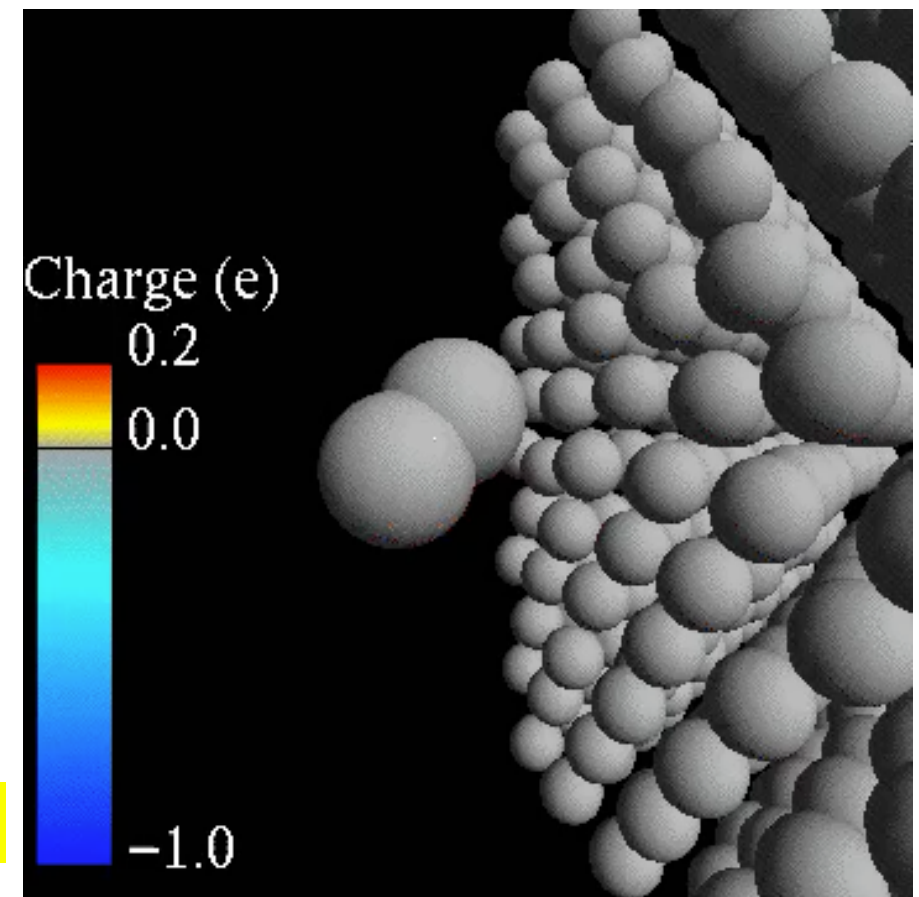


Reactive Force-Field (ReaxFF) MD: Variable N-Charge Problem

- Reactive bond order potential energy: $E_{\text{bond}}(\{r_{ij}\}, \{r_{ijk}\}, \{r_{ijkl}\}, \{BO_{ij}\})$
→ Bond breakage & formation



- Charge-equilibration (QEeq)
→ Charge transfer
Determine atomic charges $\{q_i \mid i = 1, \dots, N\}$ every MD step
to minimize $E_{\text{ES}}(\mathbf{r}^N, q^N)$ with
charge-neutrality constraint:
 $\sum_i q_i = 0$
— Dense linear system: $M q = -\chi$
 $O(N^3)!$



$$E_{\text{ES}}(\mathbf{r}^N, q^N) = \sum_i \left(\chi_i q_i + \frac{1}{2} J_i q_i^2 \right) + \sum_{i < j} \int d\mathbf{x} \int d\mathbf{x}' \frac{\rho_i(q_i; \mathbf{x} - \mathbf{r}_i) \rho_j(q_j; \mathbf{x}' - \mathbf{r}_j)}{|\mathbf{x} - \mathbf{x}'|}$$

Fast Reactive Force-Field Algorithm

- $O(N)$ fast reactive force-field (F-ReaxFF) algorithm

1) Fast multipole method

2) Temporal locality, $q_i^{(\text{init})}(t+\Delta t) = q_i(t)$

$$M q = -\chi$$

- Multilevel preconditioned conjugate gradient (MPCG) method

1) Split Coulomb matrix: $M = M_{\text{near}} + M_{\text{far}}$

2) Sparse near-field preconditioner: $M_{\text{near}}^{-1} M q = -M_{\text{near}}^{-1} \chi$

$$V_{\text{es}}(\mathbf{x}_i) = \sum_{j=1}^N \frac{q_j}{|\mathbf{x}_i - \mathbf{x}_j|}$$

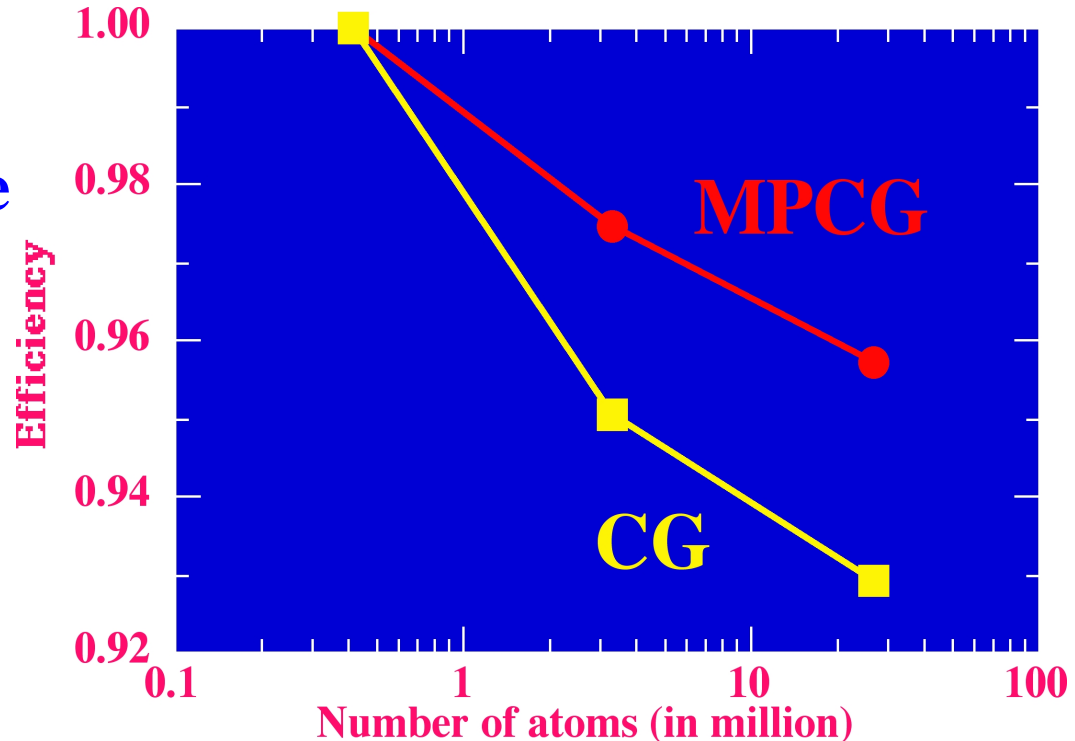
Results:

- 20% speed up of convergence

Enhanced data locality:

Improved parallel efficiency

0.93 → 0.96 for 26.5M-atom
 Al_2O_3 on 64 Power nodes



A. Nakano, *Comput. Phys. Commun.*
104, 59 ('97)

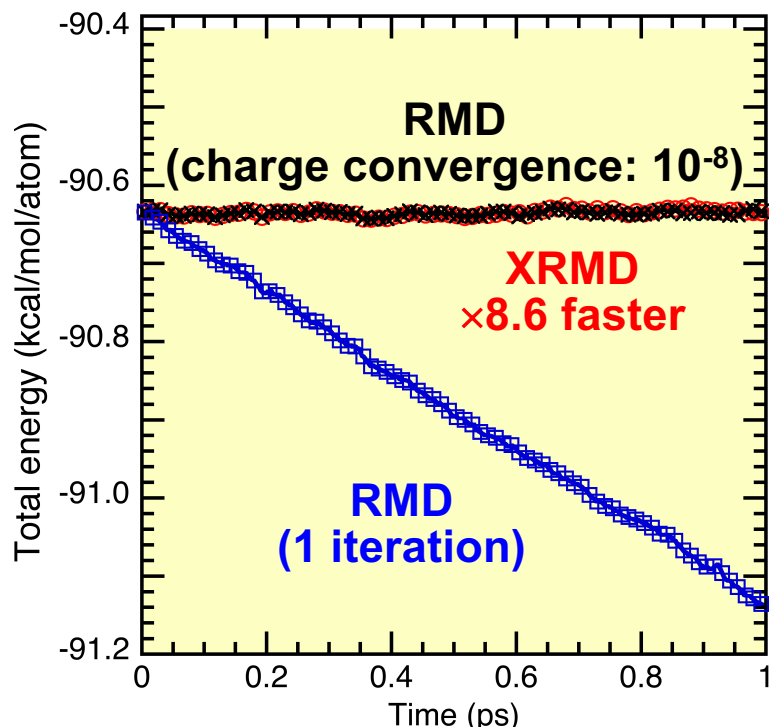
Extended-Lagrangian RMD (XRMD)

- Eliminated speed-limiting iteration for charge-equilibration in reactive molecular dynamics (RMD) by adapting an extended-Lagrangian scheme proposed for QMD [P. Souvatzis & A. Niklasson, *J. Chem. Phys.* **140**, 044117 ('14)]

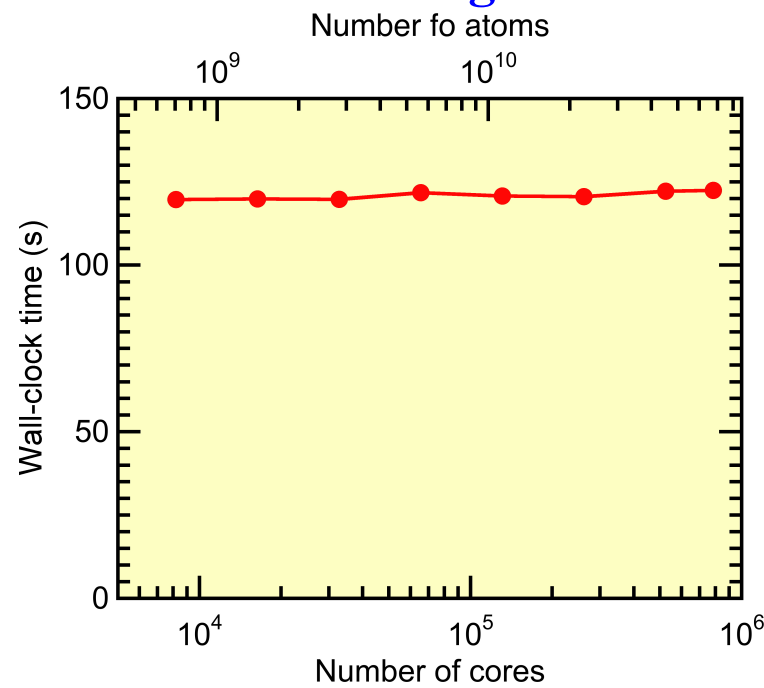
$$L_{\text{XRMD}} = L_{\text{RMD}} + \frac{\mu}{2} \sum_i \dot{\theta}_i^2 - \frac{\mu\omega^2}{2} \sum_i (\theta_i - q_i)^2$$

Auxiliary charge: dynamic variable
Physical charge

- Extended-Lagrangian RMD (XRMD) achieves the same energy conservation as fully converged RMD but an order-of-magnitude faster



Nomura *et al.*, *Comput. Phys. Commun.* **192**, 91 ('15)



- Parallel efficiency 0.977 on 786,432 Blue Gene/Q cores for 67.6 billion atoms

Quantum Molecular Dynamics (QMD)

$$M_I \frac{d^2}{dt^2} \mathbf{R}_I = -\frac{\partial}{\partial \mathbf{R}_I} E[\{\mathbf{R}_I\}, \psi(\mathbf{r}_1, \dots, \mathbf{r}_N)] \quad (I = 1, \dots, N_{\text{atom}})$$

First molecular dynamics using an empirical interatomic interaction

A. Rahman, *Phys. Rev.* **136**, A405 ('64)

$$\psi(\mathbf{r}_1, \dots, \mathbf{r}_N) \leftarrow \operatorname{argmin} E[\{\mathbf{R}_I\}, \psi(\mathbf{r}_1, \dots, \mathbf{r}_N)]$$

Density functional theory (DFT)

Hohenberg & Kohn, *Phys. Rev.* **136**, B864 ('64)

W. Kohn, *Nobel chemistry prize*, '98

$O(C^N) \rightarrow O(N^3)$
1 N -electron problem N 1-electron problems
intractable tractable

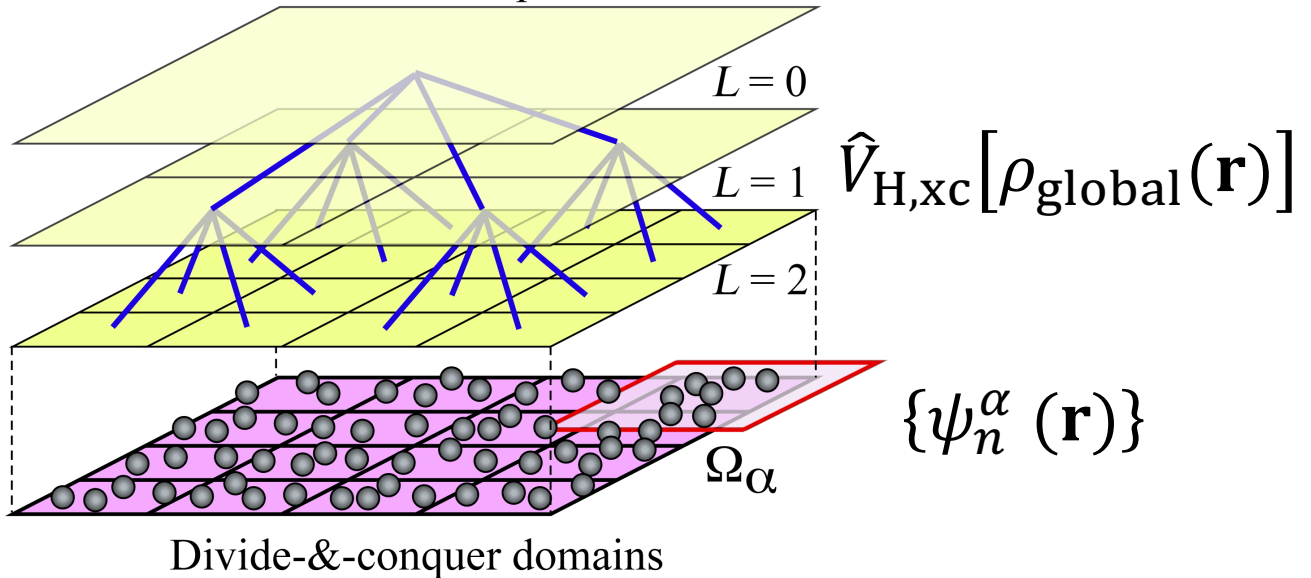
$$\psi(\mathbf{r}_1, \dots, \mathbf{r}_N) \quad \{\psi_i(\mathbf{r}) | i = 1, \dots, N\}$$

$O(N)$ DFT algorithms

- **Divide-&-conquer DFT** [W. Yang, *Phys. Rev. Lett.* **66**, 1438 ('91); F. Shimojo *et al.*, *Comput. Phys. Commun.* **167**, 151 ('05); *Phys. Rev. B* **77**, 085103 ('08); *Appl. Phys. Lett.* **95**, 043114 ('09); *J. Chem. Phys.* **140**, 18A529 ('14)]
- **Quantum nearsightedness principle** [W. Kohn, *Phys. Rev. Lett.* **76**, 3168 ('96)]
- **A recent review** [Bowler & Miyazaki, *Rep. Prog. Phys.* **75**, 036503 ('12)]

Divide-&-Conquer Density Functional Theory

Global Kohn-Sham potential



Divide-&-conquer domains

- Overlapping spatial domains: $\Omega = \bigcup_{\alpha} \Omega_{\alpha}$
- Domain Kohn-Sham equations

Global-local
self-consistent
field (SCF)
iteration

$$\left(-\frac{1}{2} \nabla^2 + \hat{V}_{\text{ion}} + \hat{V}_{\text{H,xc}}[\rho_{\text{global}}(\mathbf{r})] \right) \psi_n^{\alpha}(\mathbf{r}) = \epsilon_n^{\alpha} \psi_n^{\alpha}(\mathbf{r})$$

- Global & domain electron densities

$$\rho_{\text{global}}(\mathbf{r}) = \sum_{\alpha} p_{\alpha}(\mathbf{r}) \rho_{\alpha}(\mathbf{r})$$

Domain support function

$$\sum_{\alpha} p_{\alpha}(\mathbf{r}) = 1$$

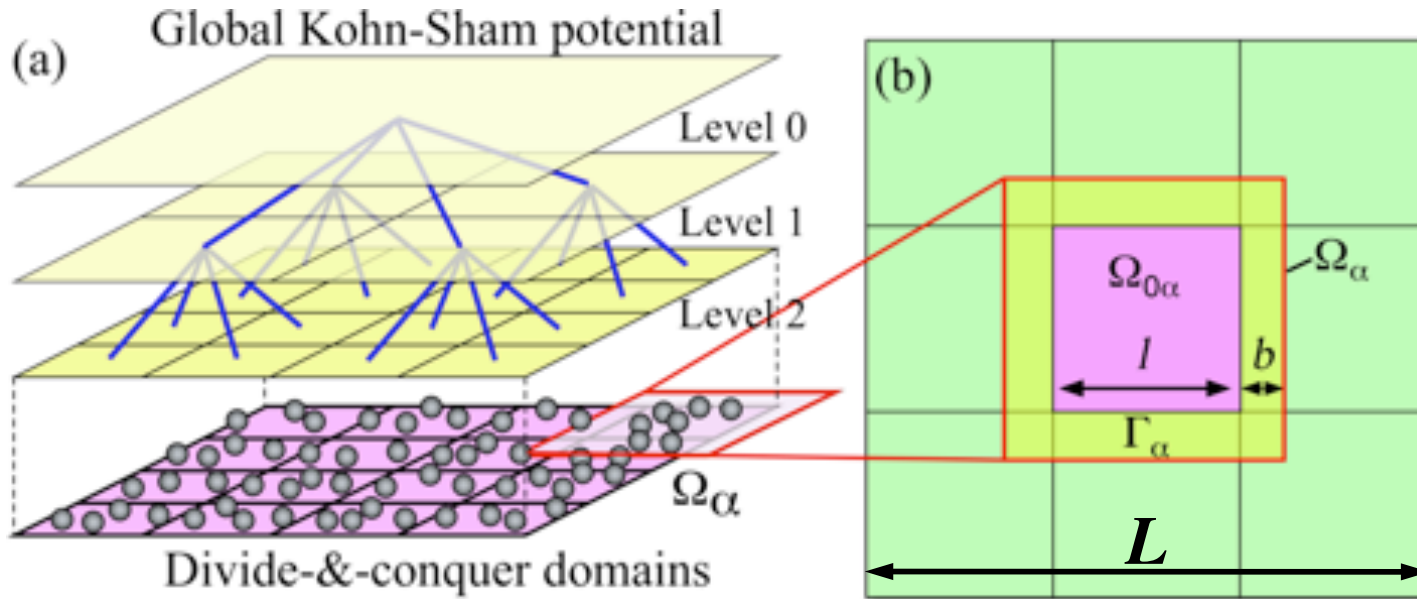
$$\rho_{\alpha}(\mathbf{r}) = \sum_n [\psi_n^{\alpha}]^2 \Theta(\mu - \epsilon_n^{\alpha})$$

Global chemical potential

$$N = \int d\mathbf{r} \rho_{\text{global}}(\mathbf{r})$$

Optimization of Divide-&-Conquer DFT

- Computational parameters of DC-DFT = domain size (l) + buffer thickness (b)



- Complexity analysis to optimize the domain size l

$$l_* = \operatorname{argmin}(T_{\text{comp}}(l)) = \operatorname{argmin}\left(\left(\frac{l}{L}\right)^3 (l + 2b)^{3\nu}\right) = \frac{2b}{\nu - 1}$$

Per-domain computational complexity of DFT = $O(n^\nu)$: $\nu = 2$ or 3 ($n <$ or $> 10^3$)

- Error analysis: Buffer thickness b is dictated by the accuracy requirement

$$b = \lambda \ln (\max \{|\Delta \rho_\alpha(\mathbf{r})| \mid \mathbf{r} \in \partial \Omega_\alpha\}) / \varepsilon \langle \rho_\alpha(\mathbf{r}) \rangle$$

Decay length

$\rho_\alpha(\mathbf{r}) - \rho_{\text{global}}(\mathbf{r})$

Error tolerance

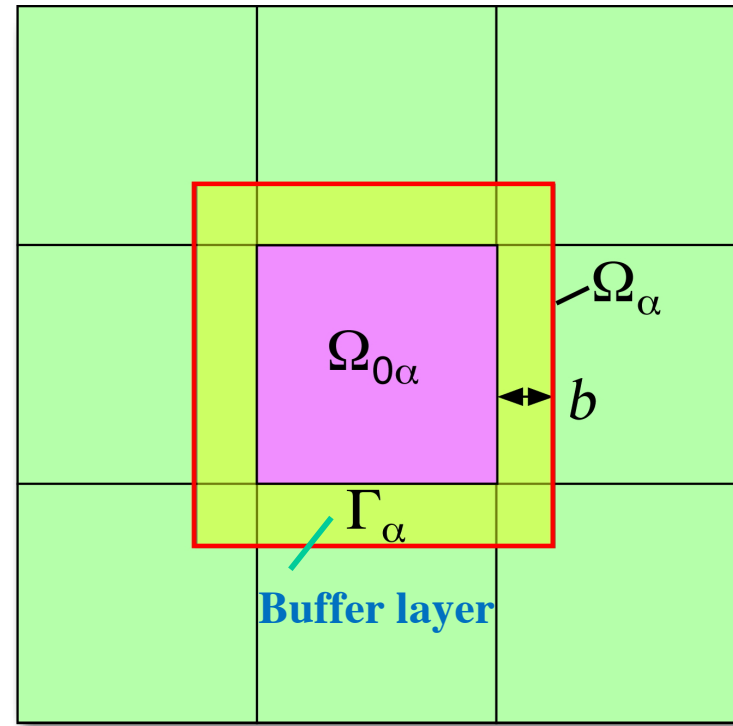
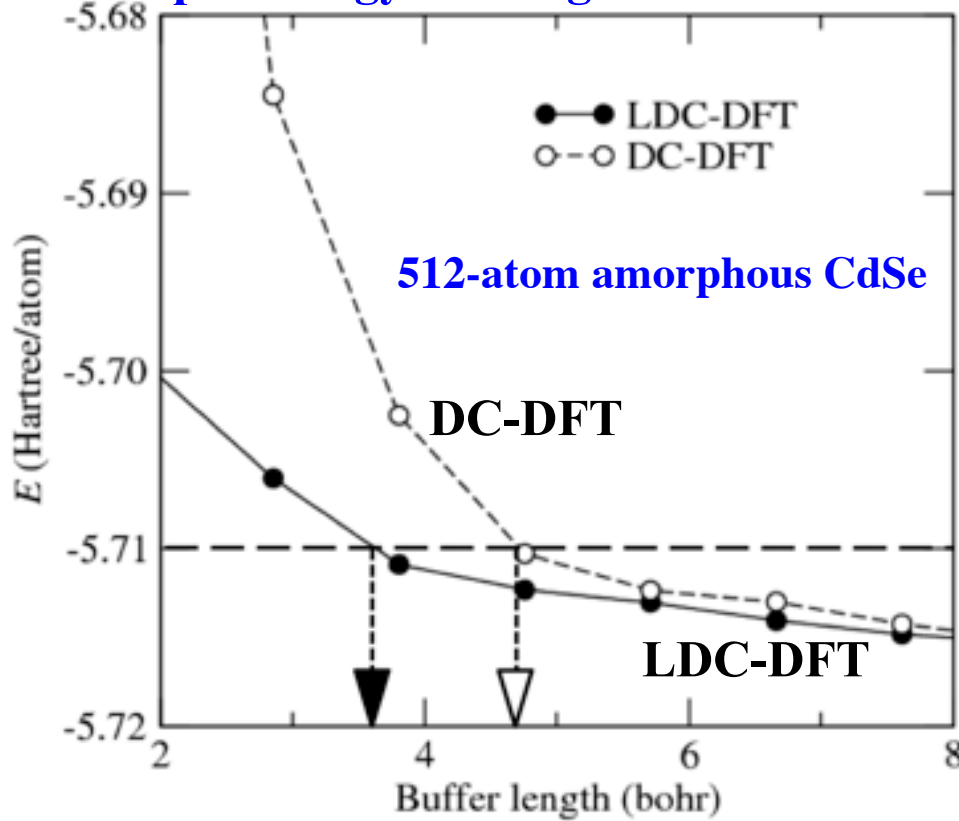
cf. quantum nearsightedness [Kohn, *Phys. Rev. Lett.* **76**, 3168 ('96)]

Lean Divide-&-Conquer (LDC) DFT

- Density-adaptive boundary potential to reduce the $O(N)$ prefactor

$$\nu_{\alpha}^{\text{bc}}(\mathbf{r}) = \int d\mathbf{r}' \frac{\partial \nu(\mathbf{r})}{\partial \rho(\mathbf{r}')} (\rho_{\alpha}(\mathbf{r}) - \rho_{\text{global}}(\mathbf{r})) \cong \frac{\rho_{\alpha}(\mathbf{r}) - \rho_{\text{global}}(\mathbf{r})}{\xi}$$

- More rapid energy convergence of LDC-DFT compared with nonadaptive DC-DFT

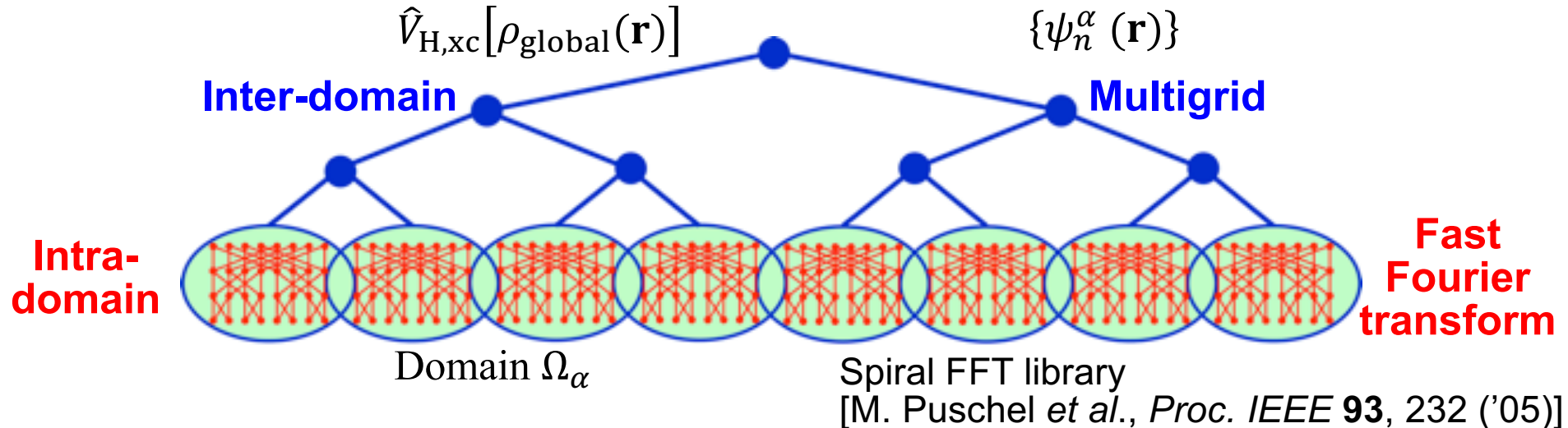


- Factor 2.03 (for $\nu = 2$) \sim 2.89 (for $\nu = 3$) reduction of the computational cost with an error tolerance of 5×10^{-3} a.u. (per-domain complexity: n^{ν})

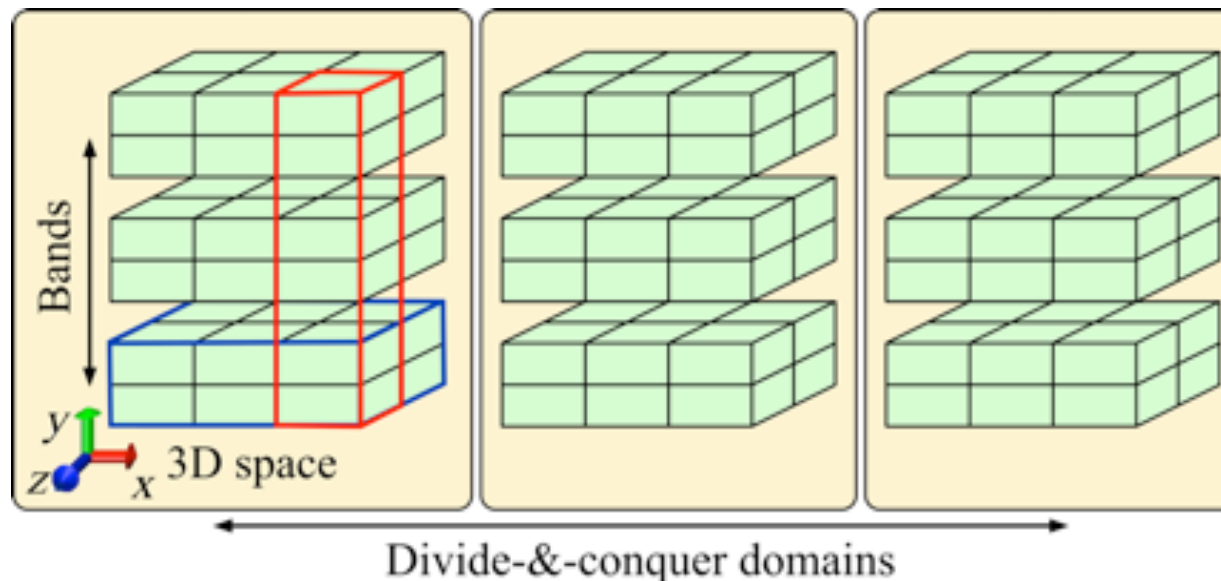
F. Shimojo *et al.*, *J. Chem. Phys.* **140**, 18A529 ('14);
Phys. Rev. B **77**, 085103 ('08); *Comput. Phys. Commun.* **167**, 151 ('05)

Hierarchical Computing

- Globally scalable (real-space multigrid) + locally fast (plane wave) electronic solver



- Hierarchical band (*i.e.* Kohn-Sham orbital) + space + domain (BSD) decomposition



Floating Point Performance

- Transform from band-by-band to all-band computations to utilize a matrix-matrix subroutine (DGEMM) in the level 3 basic linear algebra subprograms (BLAS3) library
- Algebraic transformation of computations

Example: Nonlocal pseudopotential operation

D. Vanderbilt, *Phys. Rev. B* **41**, 7892 ('90)

$$\hat{v}_{\text{nl}}|\psi_n^\alpha\rangle = \sum_I^{N_{\text{atom}}} \sum_{ij}^{L_{\max}} |\beta_{i,I}\rangle D_{ij,I} \langle \beta_{j,I}| \psi_n^\alpha \rangle \quad (n = 1, \dots, N_{\text{band}})$$



$$\Psi = [|\psi_1^\alpha\rangle, \dots, |\psi_{N_{\text{band}}}^\alpha\rangle] \quad \tilde{\mathbf{B}}(i) = [|\beta_{i,1}\rangle, \dots, |\beta_{i,N_{\text{atom}}}\rangle] \quad [\tilde{\mathbf{D}}(i,j)]_{I,J} = D_{ij,I} \delta_{IJ}$$

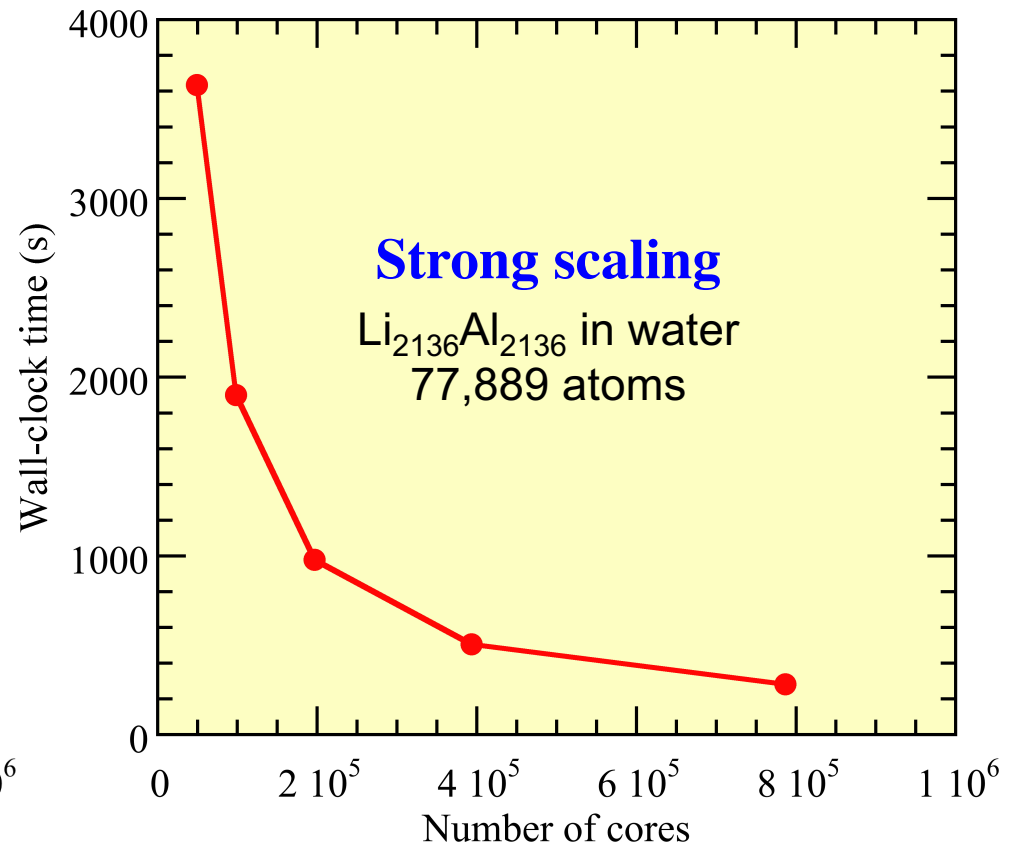
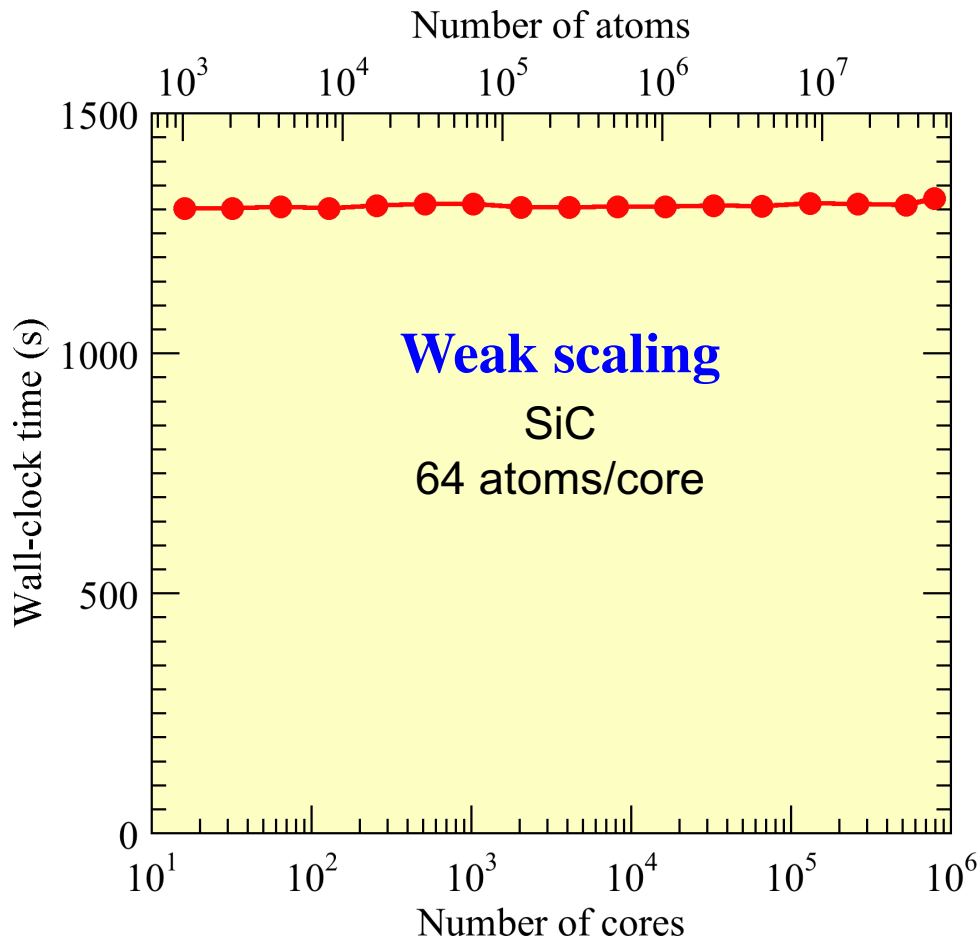
$$\hat{v}_{\text{nl}}\Psi = \sum_{i,j}^L \tilde{\mathbf{B}}(i) \tilde{\mathbf{D}}(i,j) \tilde{\mathbf{B}}(j)^T$$

- **50.5% of the theoretical peak FLOP/s performance on 786,432 Blue Gene/Q cores (entire Mira at the Argonne Leadership Computing Facility)**
- **55% of the theoretical peak FLOP/s on Intel Xeon E5-2665**

K. Nomura *et al.*, *IEEE/ACM Supercomputing, SC14* ('14)

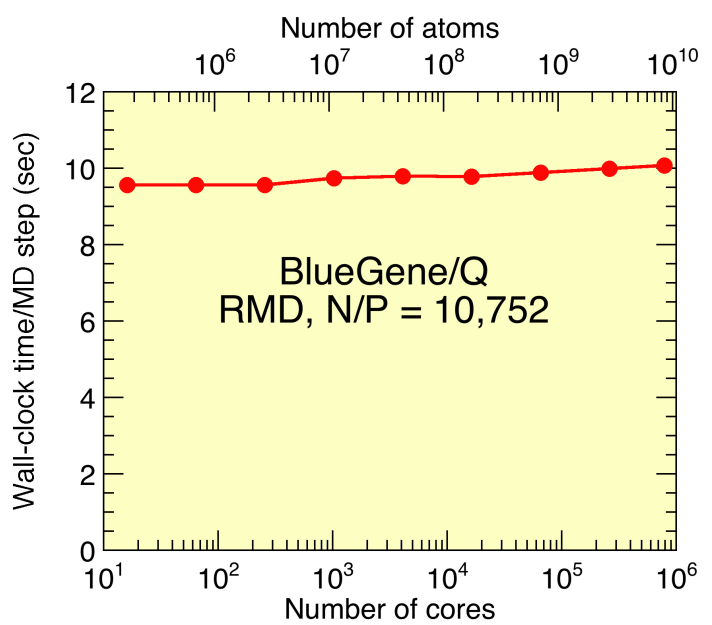
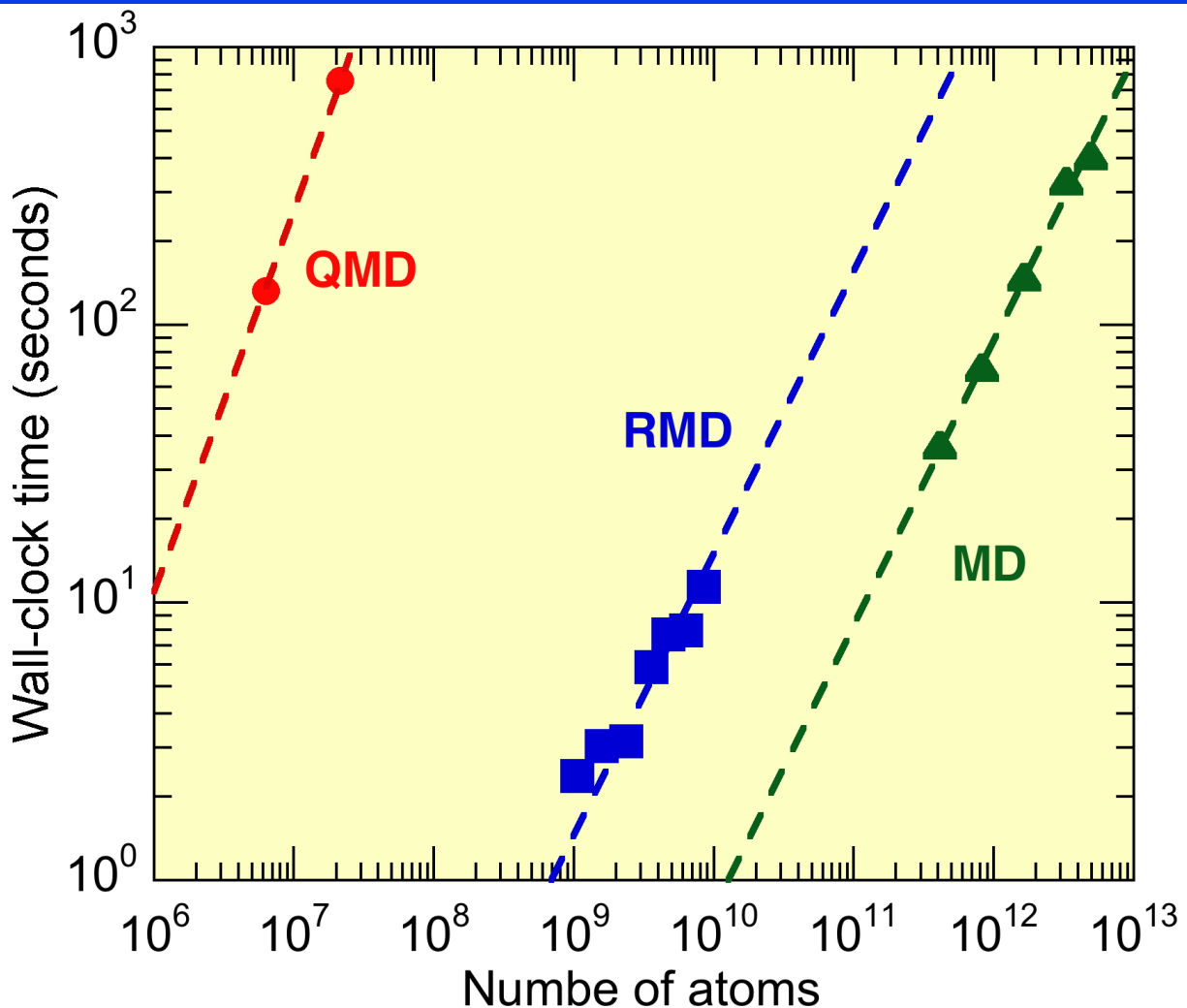
Parallel Performance

- Weak-scaling parallel efficiency is 0.984 on 786,432 Blue Gene/Q cores for a 50,331,648-atom SiC system
- Strong-scale parallel efficiency is 0.803 on 786,432 Blue Gene/Q cores



- 62-fold reduction of time-to-solution [441 s/SCF-step for 50.3M atoms] from the previous state-of-the-art [55 s/SCF-step for 102K atoms, Osei-Kuffuor et al., PRL '14]

Scalable Simulation Algorithm Suite



QMD (quantum molecular dynamics): DC-DFT

RMD (reactive molecular dynamics): F-ReaxFF

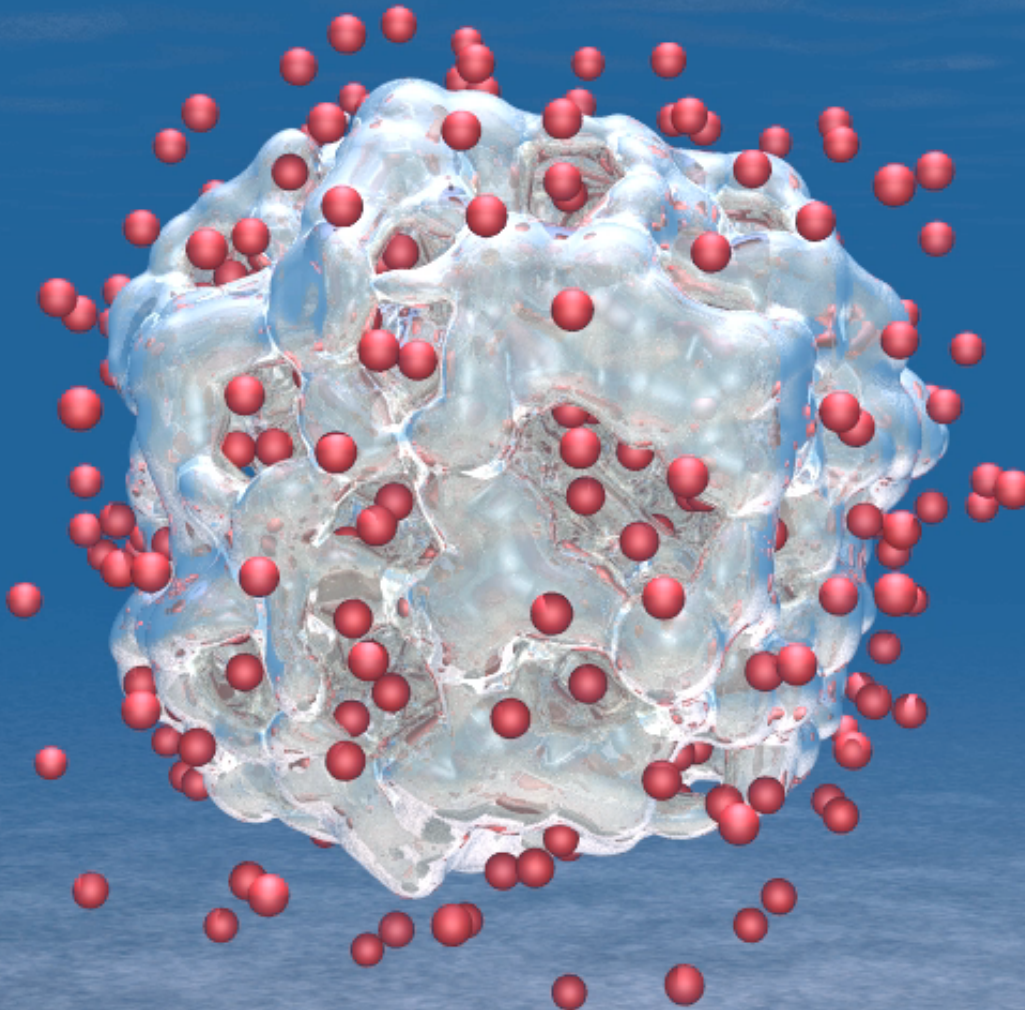
MD (molecular dynamics): MRMD

- 4.9 trillion-atom space-time multiresolution MD (MRMD) of SiO_2
 - 8.5 billion-atom fast reactive force-field (F-ReaxFF) RMD of RDX
 - 1.9 trillion grid points (21.2 million-atom) DC-DFT QMD of SiC
- parallel efficiency 0.98 on 786,432 BlueGene/Q cores

H₂ Production from Water Using LiAl Particles

16,661-atom QMD simulation of Li₄₄₁Al₄₄₁ in water
on 786,432 IBM Blue Gene/Q cores

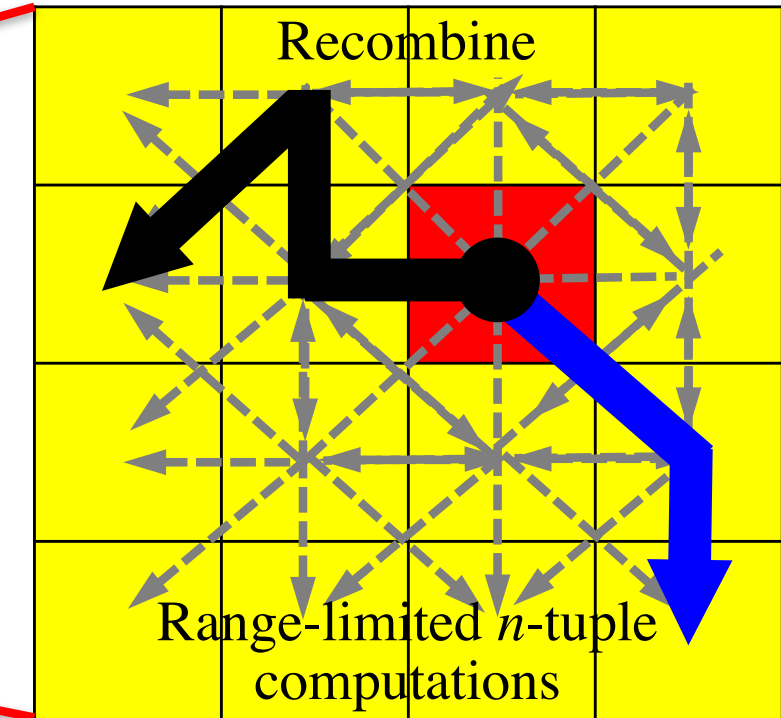
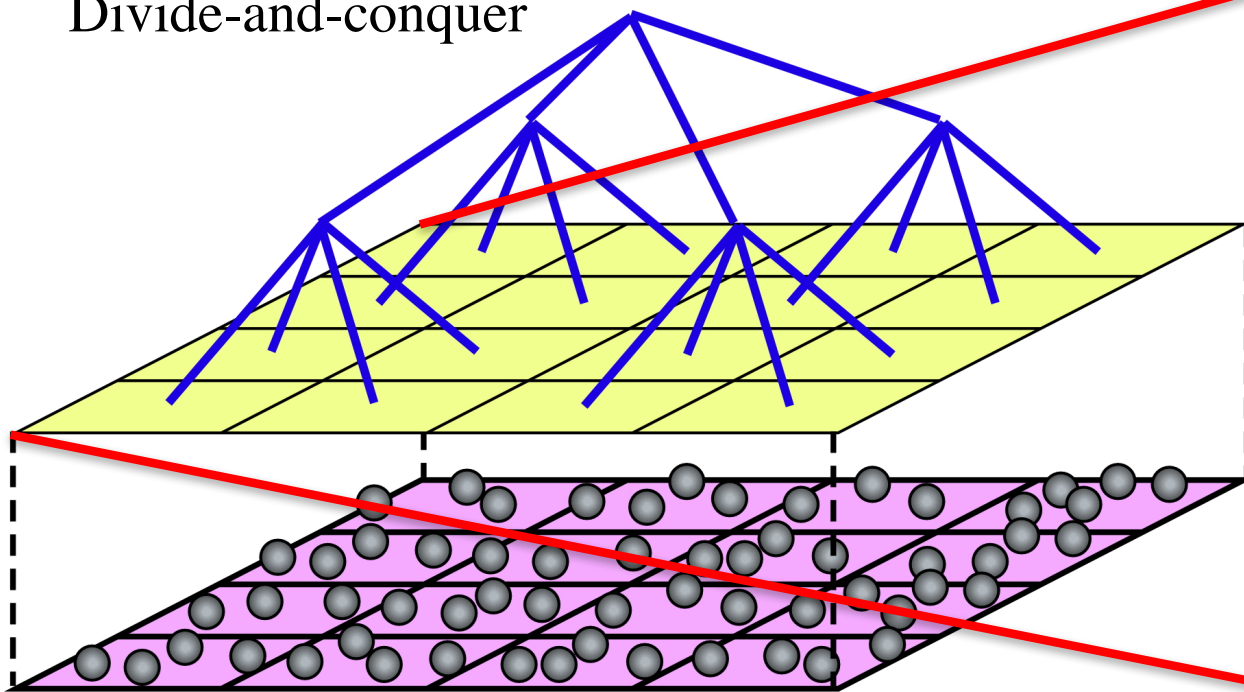
K. Shimamura *et al.*,
Nano Lett. **14**, 4090 ('14)



21,140 time steps (129,208 self-consistent-field iterations)

Divide-Conquer-Recombine Algorithms

Divide-and-conquer



M. Kunaseth et al., ACM/IEEE SC13 ('13)

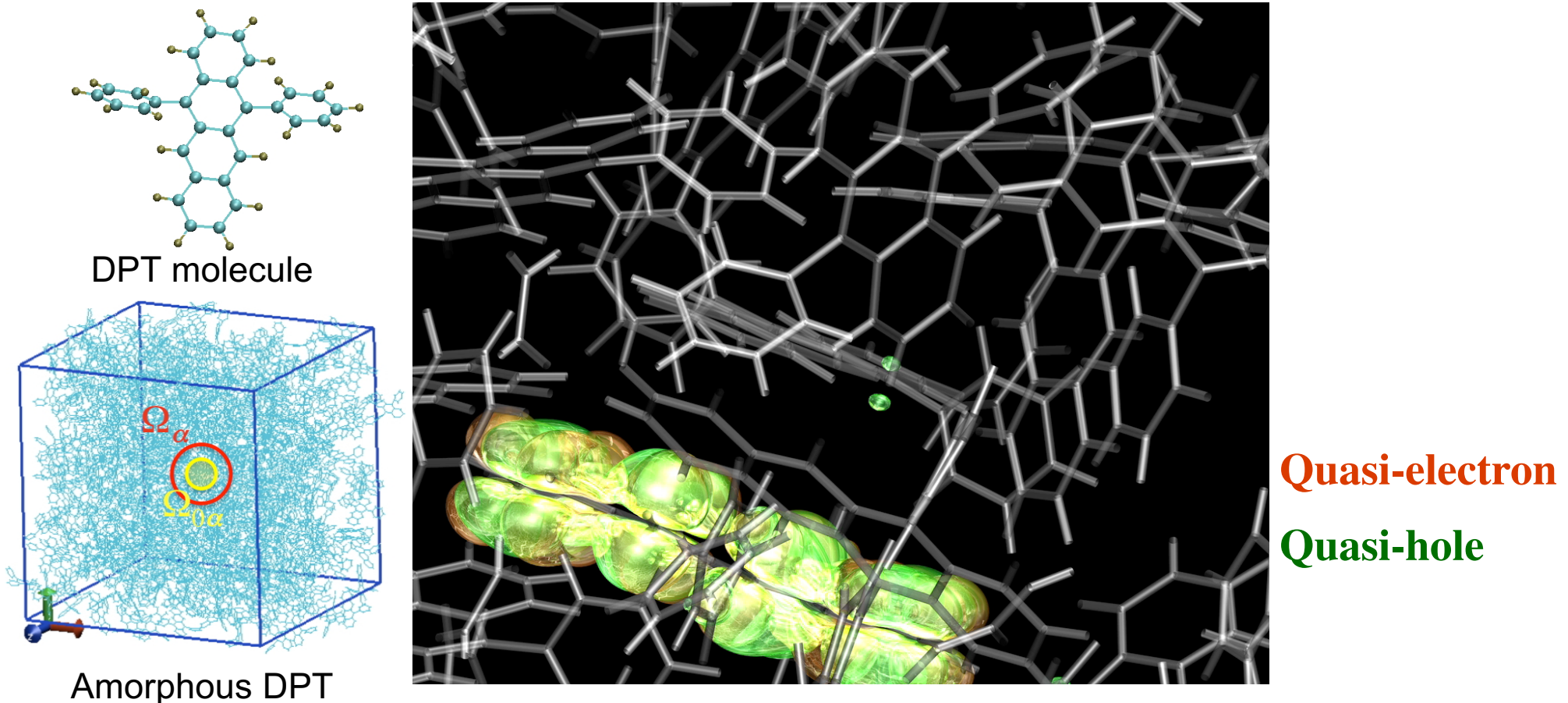
Globally informed local DC-DFT solutions are used in the recombine phase as compact bases to synthesize global properties in broad applications:

- High-order inter-molecular-fragment correlation [S. Tanaka et al., '13]
- Global frontier orbitals (**HOMO & LUMO**) [S. Tsuneyuki et al., '09, '13]
- Global charge migration [H. Kitoh-Nishioka et al., '12; C. Gollub et al., '12]
- Global exciton dynamics [W. Mou et al., '13]

F. Shimojo et al., J. Chem. Phys. **140**, 18A529 ('14); K. Nomura et al., IEEE/ACM SC14 ('14)

Singlet Fission in Amorphous DPT

- Photo-current doubling by splitting a singlet exciton into 2 triplet excitons
- Singlet fission in mass-produced disordered organic solid → efficient low-cost solar cells
- Exp'l breakthrough: SF found in amorphous diphenyl tetracene (DPT)



- Divide-conquer-recombine nonadiabatic QMD (phonon-assisted exciton dynamics) + time-dependent perturbation theory (singlet-fission rate) + kinetic Monte Carlo calculations of exciton population dynamics in 6,400-atom amorphous DPT